Journal of Applied Fluid Mechanics, Vol. 12, No. 3, pp. 971-980, 2019.
Available online at www.jafmonline.net, ISSN 1735-3572, EISSN 1735-3645.
DOI: 10.29252/jafm.12.03.29037

Convective Heat Transfer between Liquid Argon Flows and Heated Carbon Nanotube Arrays using Molecular Dynamics

T. M. Thomas and N. Vinod†

Department of Mechanical Engineering, Indian Institute of Technology Gandhinagar, Palaj, Gujarat-382355, India

†Corresponding Author Email: vinod@iitgn.ac.in

(Received March 23, 2018; accepted September 22, 2018)

ABSTRACT

This paper presents the molecular dynamics simulations of unconfined forced convective flow through the nanostructures at steady state condition. A better understanding of forced convective flow through the nanostructures is important because of its wide range of applications in nano-scale devices. Present work focuses on the heat transfer process of argon flow over a carbon nanotube and carbon nanotube arrays with constant surface temperature using molecular dynamics simulations. We consider two elementary configurations for the case of carbon nanotube arrays based on the unit cell structure. The simulation domain consists of fixed carbon nanotubes surrounded with the flowing argon atoms. An extensive study of momentum and thermal transport between carbon nanotube and surrounded argon atoms are analyzed from its microscopic state. The heat transfer coefficient is found in the order of 10^8 W/m^{2}K. The method proposed in this paper can be an elementary step for the geometry calculation of nano-structured heat sink in the high heat flux electronic chips.

Keywords: CNT arrays; Heat transfer; Convection.

1. INTRODUCTION

The amount of heat produced from the micro-electronic equipment has a steep upward jump in the past few years. Modern electronic devices are encountered with a heat flux in the range of 50 MW/m^2 or even higher and the nanometer-sized transistors (Karayiannis and Mahmoud, 2017). As a result, heat management of these devices becomes a great challenge to the researchers. This problem was first identified by Tuckerman and Pease (Tuckerman and Pease, 1981) in 1981 by providing a microchannel heat sink, as an integral part of the electronic equipment. Boiling (Incropera, 2007) can be considered as the most efficient heat transfer method in various cooling devices and energy conversion systems. Boiling allows high heat flux at low wall superheat. In recent years, researchers have tried to increase the critical heat flux (CHF) of the boiling system, and also to develop efficient heat-transfer fluids. Because of the superior thermal and electrical properties researchers are attracted with nano-fluids as a coolant which are the suspension of nanometersized solid particles. An enhancement in critical heat flux occurs during the nano-fluid boiling process (You, Kim and Kim, 2003). But the actual reason for the CHF enhancement is due to the formation of nano-particle deposition on the heated surface. So it has been concluded that instead of boiling by nano-fluid, it is better to coat the surface with nano-particles for the enhancement of CHF (Barber, Brutin and Tadrist, 2011). Because of the exceptionally higher thermal conductivity, the carbon nanotube (CNT) has attracted great interest on nano-fin applications (Berber, Kwon and Tománek, 2000).

The heat energy in a carbon nanotube is transported by the propagating strong lattice vibrations and intrinsic properties of the strong sp2 lattices (Balandin, 2011). The structure of CNT is similar to the graphene sheet but as compared to them CNT shows different quantization for phonon modes and larger curvature. The heat transfer mechanism in a single wall CNT is categorized into three different regimes named as ballistic, diffusive and transition regimes (Ho, Chen, Wen, Yang, and Lee, 2016). In ballistic regime, the nanotube length is smaller than the mean-free path length. So the thermal resistance due to the phonon-boundary scattering dominates over phonon-phonon scattering. If the carbon nanotube length is more than the diffusion length, the heat is transported mainly by diffusion mechanism

and the phonon-boundary scattering is negligible as compared with phonon-phonon scattering. In the transition regime, the length of the carbon nanotube is lies between mean free path and diffusion length so both the mode of scatterings are significant in this regime. From experiments, the mean free path length of single wall CNT at room temperature is reported as 500- 750 nm (Kim, Shi, Majumdar and McEuen, 2001; Yu, Shi, Yao, Li and Majumdar, 2005). The non-equilibrium molecular simulation shows the dependence of phonon frequency on the mean free path length of CNT. At room temperature, the mean free path length becomes more than 10 μm for low-frequency phonons of below 0.5 THz (Sääskilahti, Oksanen, Volz and Tulkki, 2015).

The fluid surrounding a heated nano-particle can be heated above its boiling point without the presence of phase change (Merabia, Keblinski, Joly, Lewis and Barrat 2009). So miniature sized single-phase cooling systems can be designed to remove high heat fluxes effectively from the modern electronic devices. It avoids some of the major difficulties associated with the two-phase flow systems like flow instabilities, requirement of low saturation temperature working fluid, flow reversal, rapid bubble expansion (Kandlikar, 2005). The interfacial resistance between the wall boundary and the working fluid has a major role in the heat transfer efficiency of nano-sized cooling devices. Various theoretical studies were conducted using molecular dynamics to understand the interfacial transport between the wall and working fluid (Barisik and Beskok 2012). Rabani *et al.* have investigated the effect of channel width confinement on the heat transfer characteristics in the nano-channel (Rabani, Heidarinejad, Harting and Shirani 2018). They found that the fraction of interfacial resistance (ratio of interfacial resistance to the total thermal resistance) increases as the channel size decreased. The effect of flow velocity in a nano-channel was investigated by Liu *et al.* and concluded that interfacial resistance decreases with increase in streaming velocity (Liu, Fan, Zhang, Yuen and Li, 2010). The interfacial resistance needs to be controlled in a nano-scale devices to resolve the thermal management issues associated with these devices. A comprehensive review of Zhang *et al.* discusses the interfacial transport mechanism and factors influencing interfacial resistance at the nano-scale (Zhang, Yuan, Jiang, Zhai, Zeng, Xian, Qin and Yang, 2018). They also presented the different available techniques can be employed in nano-scale devices for reducing the interfacial resistance.

Although carbon nanotube has exceptionally well thermal conductivity property, the actual heat transfer enhancement is limited because of the interfacial resistance offered between the CNT and liquid matrix molecules in the CNT based nano-scale devices. Interfacial thermal transport mechanism between CNT and matrix molecules is very complex and more studies are required to design the CNT based nano-scale devices. The interfacial resistance strongly depends on the type of matrix and the van der Wall forces between nanotube and matrix. It is found that as the diameter increases, the interfacial thermal conductivity of carbon nanotube also increases, which saturates when the carbon nanotube has a diameter larger than 1.4 nm, corresponds to (10, 10) nanotube (Xu and Buehler, 2009). The values reported for the interfacial resistance vary from 0.76×10^{-8} to 20×10^{-8} m^2K/W (Singh, Unnikrishnan, Banerjee and Reddy, 2011). Modelling and simulation of nano-scale heat transport can be done using molecular dynamics (MD) simulation where the time evolution of a set of interacting particles are followed by solving their equations of motion (Allen and Tildesley, 1989).

Dispersion of nano-structures can be managed in advance through design and manufacturing. The attachment of aligned single-walled carbon nanotube (SWCNT) over the silicon surface has successfully developed by Jinxian Yu (Yu, Shapter, Quinton, Johnston and Beattie, 2007). The common feature in these materials is that one nano-structured unit can be identified as the building block. There are so many questions has to be answered related to the nano-fins attachment to a solid surface, like, how the nano-fins are to be arranged? What is the optimum thickness of coating? From the experiments, it is found that when the characteristic length decreases, the heat transfer behavior shows different trends (Wu and Cheng, 2003). Numerous researchers have investigated fluid flow through nano-channel using MD techniques. There are different methods for generating fluid flow in a channel, widely accepted method for generating fluid flow is by applying a large force to each atom present in the channel (Prabha and Sathian, 2012). The above method doesn't work for convective heat transfer simulation because the applied external force continuously supplies artificial energy to the simulation domain which can alter the temperature of the system. The periodic boundary condition is no longer applicable for convective heat transfer simulation (Alexiadis and Kassinos, 2008) since the fluid temperature is varied along the direction of flow during convection, which is not a periodic boundary condition.

Markvoort *et al.* (Markvoort, Hilbers and Nedea 2005) suggested a method for simulating convective heat transfer in which the external force is applied only to the inlet atoms and temperature reset of atoms across the outlet is carried out by thermostatting. The drawback of this method is explained by the Song Ge *et al.* (Ge, Gu and Chen, 2015) and they proposed an improved method for simulating convective heat transfer problems in nanochannel by first applying an external force to the inlet atoms continued by thermosetting to the desired temperature by subtracting the center-of-mass velocity, subsequently adding the subtracted velocity in the first step. This study focusing on the investigation of heat transfer analysis of carbon nanotube with the surrounding fluids. A methodology has been proposed here for investigating the unconfined steady-state convective flow simulations.

The present work comprised of two cases. In the first case, the interfacial resistance present in the interface of carbon nanotube and argon atoms is investigated based on lumped heat capacitance approach. In the

second case, the convective heat transfer analysis of argon flow around the carbon nanotube as well as the different configurations of carbon nanotube arrays have been investigated. The current work aims to study the heat removal from an array of heated nanotubes keeping an objective to enhance the heat transfer rate from a surface. We study two different configurations and study the heat transfer in those configurations. We perceive this as a primary step forward to enhancement of heat removal from an object, e.g. computer chips.

2. COMPUTATIONAL METHOD

The whole computations are carried out by solving Newton's laws of motion using the molecular dynamics package LAMMPS (Plimpton, Crozier and Thompson 2007). Single wall carbon nanotubes are the tube shaped rolled structures of graphene sheet as shown in Fig. 1. The structure of a CNT changes accordance with the rolling direction. The corresponding direction vector is termed as chiral vector (C_h) and defined by,

$$C_h = na_1 + ma_2 \tag{1}$$

where a_1 and a_2 are the unit cell vector, (n,m) are the positive integers. The chiral vector for a (n,m) type CNT is drawn by connecting two carbon atoms of (0,0) and (n,m) as illustrated in Fig. 1. In all MD simulations, 60 A◦ long arm-chair type single wall carbon nanotube with a chirality of (10,10) and liquid argon atoms with a density of 1400 kg/m3 is considered. The atomic mass of argon and carbon atoms are 39.94 amu and 12 amu respectively. The C-C interaction in a carbon nanotube composed of bonded interaction and long-range van der Wall force. The potential energy associated with C-C bonded interaction includes bond stretching potential, angle potential and torsional potential. The C-C interaction of CNT is modelled using Adaptive Intermolecular Reactive Empirical Bond Order (AIREBO) potential since it is considering the long-range interaction along with bonded interaction (Stuart, Tutein and Harrison 2000).

The pair interaction between Ar-Ar and Ar-C are modeled with 12-6 Lennard-Jones (LJ) potential (Jones, 1924) with a cut-off distance of 10 A° is given by,

$$U_{l-j} = 4\varepsilon\left[\left(\frac{\sigma}{r_{ij}}\right)^{12} - \left(\frac{\sigma}{r_{ij}}\right)^{6}\right] \tag{2}$$

where r_{ij} is the inter-atomic distance between Ar-Ar and Ar-C pairs, ε is the depth of the potential well and σ is the distance at which the potential becomes zero. The L-J parameters for the pair interactions are $\varepsilon_{Ar-Ar} = 1.66 \times 10^{-21}$ J and $\sigma_{Ar-Ar} = 3.405$ A°. The L-J parameters for Ar-C pair interaction can be approximated by Lorentz-Berthelot mixing rule (van Gunsteren, Weiner and Wilkinson, 2013) by considering L-J parameters for C-C pair interactions as $\varepsilon_{C-C} = 0.384 \times 10^{-21}$ J and $\sigma_{C-C} = 3.21$ A°. The C-C bond length in the CNT is 1.421 A° and a cut-off distance of 6 A° is considered for AIREBO potential. A timestep of 1 f s is used for the time integration in all simulations.

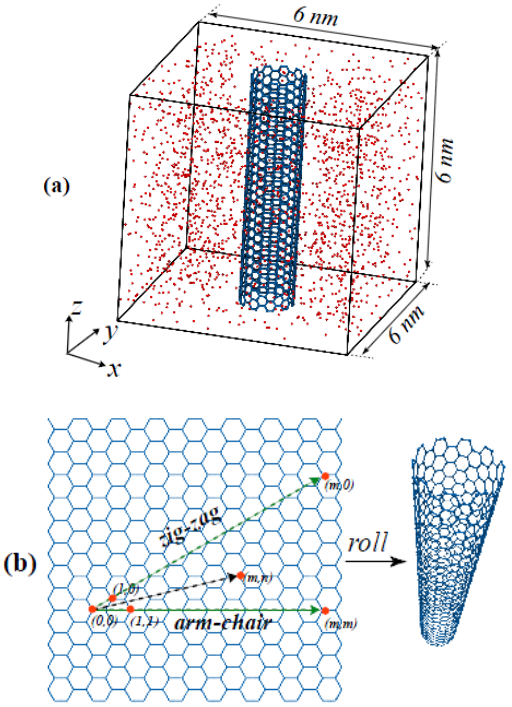

Fig. 1. (a) A snap shot of computational domain for the computation of interfacial resistance-CNT of 6 nm length with (10,10) chirality surrounded with 4000 argon atoms (b) Schematic structure of arm-chair CNT of (10,10) chirality.

2.1 Computation of Interfacial Resistance

Figure 1 represents the computational model, where centrally placed heated arm-chair carbon nanotube surrounded with 4000 liquid argon atoms with a density of 1400 kg/m3. It numerically models a system with a heated carbon nanotube and surrounded liquid argon particles in micro-canonical (NVE) and canonical ensemble (NVT) at 300 K. The axis of the carbon nanotube is aligned with z-axis and the box dimension is $60 \times 60 \times 60$ $A^{\circ 3}$. The temperature gradient within the carbon nanotube can be neglected because of the extremely high thermal conductivity. In the case of unsteady heat transfer between the carbon nanotube and argon atoms, the carbon nanotube can be considered as the lumped body. It is reported that temperature difference between the carbon nanotube and the matrix molecules follows exponential decay (Clancy and Gates, 2006).

The initial structure has been prepared using Packmol (Martínez, Andrade, Birgin and Martínez, 2009). It randomly places the atoms in a box and there are some atoms very closely or overlapped with the other atoms. Minimization is carried out for relaxing the initial structure created from the Packmol. After minimization, the velocity of each atom is randomly assigned based on Gaussian distribution at a temperature of 300 K. Then the

whole system is relaxed in NVE ensemble for 500 ps. During this relaxation step the kinetic energy is converted to potential energy, which keeps the system temperature lower than 300 K. In the next step, the system is equilibrated at a temperature of 300 K in NVT ensemble. This simulation also runs around 1500 ps. Here the thermostatting is achieved using Nose-Hoover thermostat. After the full equilibration of the system at 300 K, the temperature of the carbon nanotube have increased to 500 K by the direct velocity rescaling. At that moment system is no more in the equilibrium state. The energy from the carbon nanotube is transported to the argon atoms when the system is coupled with NVE ensemble. These simulations are continued till the argon and carbon nanotube temperatures become converged. The interfacial thermal resistance R_K can be derived from the lumped heat capacitance approach in transient heat conduction, which is given by

$$mC\frac{dT}{dt} = \frac{A_s}{R_K}(T - T_\infty) \tag{3}$$

where m is the mass of the carbon nanotube, C is the heat capacity, A_s is its surface area, T_∞ is the average temperature of the surrounding argon fluid and T is the average temperature of the carbon nanotube at a time of t seconds. Integrating the Eq. 3 from t=0 to t, we get

$$\Delta T(t) = \Delta T_{initial} \exp(\frac{-t}{\tau}) \tag{4}$$

The time constant is represented with τ which signifies the rate of exponential decay. The interfacial resistance can be computed from the time constant value τ, given by

$$R_k = \frac{\tau}{B} \tag{5}$$

As per literature the quantity $B = \frac{mC}{A_s}$ is constant for a carbon nanotube (Huxtable, Cahill, Shenogin, Xue, Ozisik, Barone, Usrey, Strano, Siddons, Shim, *et al.* 2003) and which is equal to 5.6×10^{-4} J/m^{2}K.

2.2 Argon Flow over a CNT and CNT Arrays

Modelling of convective heat transfer in MD is very tedious because of difficulties in simultaneous controlling of temperature and velocity. Figure 2 represents the complete simulation setup considered for the argon flow over a CNT. A spring force is applied to each nanotube to tether them at the initial centre of mass throughout the simulations. A spring constant of 800 N/m is assumed here for considering the effect of driving force acting on the CNT from argon atoms. The supplied spring energy is excluded from the total potential energy calculation of the system. The whole simulation box contains 4 blocks. The block represented from x = 0 A° to x = 60 A° is the actual simulation region, where the MD integrations were carried out and the dimension of the domain is $60 \times 60 \times 60$ $A^{\circ 3}$. At the left side of the inlet section, extra three artificial regions are constructed with names A, B and C. These three artificial regions make it possible for to generate the uniform flow with uniform temperature boundary condition at inlet section.

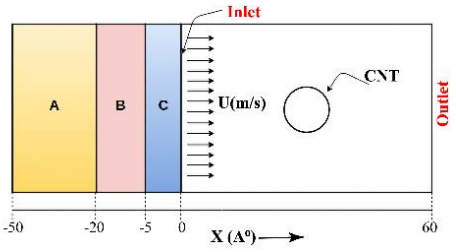

Fig. 2. Schematic of computational domain for argon flow over the CNT with three artificial regions represented as A (Region for deleting past history data by Langevin thermostat), B (Region were external force is applied) and C (Region for temperature resetting).

The external force in the direction of x-axis is applied at the region B, which providing an equal force to every atom in the region B, which generates a pressure driven type flow. The amount of force required to generate the uniform flow is approximately calculated by trial and error method after checking the inlet velocity for different force magnitudes. So an external force of 6×10^{-14} N is applied to all the atoms in the region B for making a uniform flow of 15 m/s at the inlet section. In region C the temperature reset has been carried out after subtracting the center of mass velocity. After the temperature reset, the removed center of mass velocity added back to the atoms. The inlet particles have a memory of their past history which alter the initial uniform flow condition at the inlet section when the simulations are running for a long time. Artificial filter A has created at the leftmost area for resolving this problem. It will receive all the outlet particles and prevent passage of all pressure disturbances, while transmitting atoms, fully equilibrated, at the desired flow rate. This is achieved by thermostatting with a strongly-coupled Langevin thermostat (Schneider and Stoll, 1978) and a streaming velocity, which removes their past history details and fresh particles were supplied into the simulation box. A timestep of 0.1 f s is used for the Langevin thermostating. This region should be too wide, a few multiples of force cut-off. Here a 30 A° wide region is considered. The instantaneous average velocity normal to the flow direction across each sub-regions was calculated at the inlet section and the value was found to be in the order of 15 ± 0.5 m/s. This ensures that combined effect of these three operations by creating three artificial regions near to the inlet section of the computational domain was able to provide a uniform flow at the inlet section by erasing all the past history of atoms because of periodic boundary condition.

Initially, the whole system is equilibrated in NVE ensemble at 300 K for 0.5 million timesteps, followed by an NVT dynamics for 2.5 million steps. After equilibration, an external force has applied in the region B. The temperature reset in the sub-region of C have implemented using Berendsen thermostat

(Berendsen, Postma, van Gunsteren, Di-Nola and Haak, 1984) after subtracting the mean flow velocity. The Langevin thermostat has applied in the region A for deleting the past history of outlet particles. After applying all these dynamics the temperature of carbon nanotube have been increased to 600 K by direct velocity scaling, it is continued at each timestep for maintaining the constant temperature condition of the carbon nanotube. Then 15 million timesteps are simulated for reaching the steady state condition. Finally, another 10 million timesteps are used for statistical sampling. The velocity and the temperature distribution can be found by dividing the whole simulation box into small lattices of dimension $4 \times 4 \times 60\ A^{\circ 3}$. The velocity at each sub-regions is computed by averaging the mean velocity of each sub-region. The temperature is computed based on averaging thermal velocity of all atoms in each sub-regions after the subtraction of mean velocity from the molecular velocity, as per the following equation

$$T = \frac{1}{3Nk_B}\sum_{j=1}^{N} m_j (v_j - \bar{v}_{avg})^2 \tag{6}$$

To compute heat transfer coefficient, a region is defined around the nanotube with a dimension of 20 × 20 × 60 $A^{\circ 3}$ is considered, which can be mathematically defined as,

$$h = \frac{q_{avg}}{T_w - T_{avg}} \tag{7}$$

Here q_{avg} is the average heat flux of the defined region and T_{avg} is the average temperature of the defined region. T_w is the surface temperature of the carbon nanotube, which is equal to 600 K.

The heat flux value in Eq. 7 is computed from the equation,

$$q = \frac{1}{V}\left[\sum_j e_j v_j - \sum_j S_j v_j\right] \tag{8}$$

where V is the volume of the region considered, e_j is the per-atom energy (kinetic and potential energy), v_j is the velocity of the atom j and S_j is the per-atom stress tensor based on the definition given by Heyes (Heyes, 1994).

Figure 3 represents two different configurations of carbon nanotube arrays based on the angle between the direction of flow and a line connecting the centers of two nanotubes in adjacent rows. From the geometric structure of these nano-structured surfaces, a repetitive unit cell can be identified on each configuration as illustrated in Fig. 3. In both the cases, each unit cell consists of four carbon nanotube. Based on the angle, the investigation has been conducted for 45° and 90° configuration with a uniform temperature and velocity profile at the inlet. In the actual case, the uniform velocity and temperature profile at the inlet of a unit cell changes when it passes through each unit cell. However, the numerical simulations were carried out by neglecting the effect of inlet velocity and temperature profile on the average heat transfer coefficient value at steady state condition.

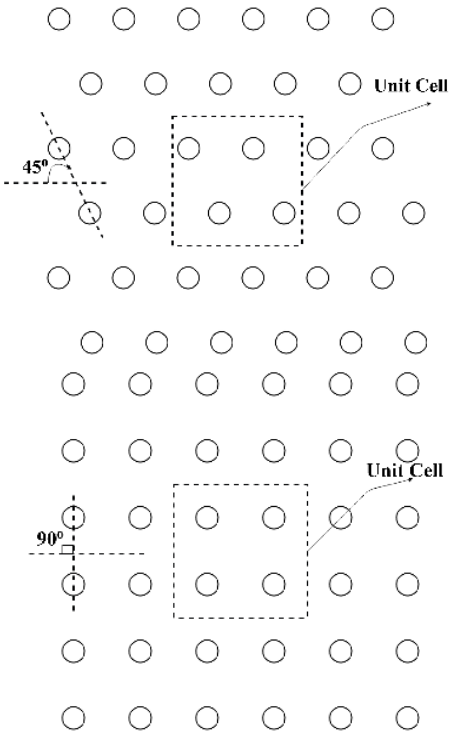

Fig. 3. Schematic representation of two different configurations of CNT arrays over a plane surface with an identified unit cell. Top: 45° configuration and bottom: 90° configuration.

The convective heat transfer in argon flow over the CNT arrays can be investigated using the same methodology as explained in the case of argon flow around the CNT. The simulation box having a dimension of 90 × 90 × 60 $A^{\circ 3}$ in both the configurations. In the simulation domain, the simulation box center can be considered as the origin. Four carbon nanotubes are placed with centres (-15,15,0), (15,15,0), (-15,-15,0) and (15,-15,0) A° for the 90° configuration. In the 45° configuration, carbon nanotubes placed at (-22.5,15,0), (7.5,15,0),(-7.5,-15,0) and (22.5,-15,0) A°. The temperature of each CNT is maintained at 600 K. For the calculation of temperature and velocity distribution, 6 × 6 × 60 $A^{\circ 3}$ blocks are considered and for heat transfer coefficient, a box of 30×30×60 $A^{\circ 3}$ is defined around each carbon nanotube.

3. RESULTS AND DISCUSSIONS

This section presents the important results obtained from the computational study of heat transfer between CNTs and surrounded Ar atoms by molecular dynamics approach. Conduction and convection studies between CNTs and surrounded Ar atoms is investigated with two different set of simulations and

results are presented in the following subsections.

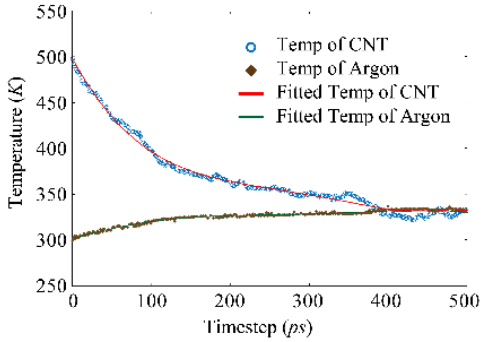

Fig. 4. Variation in average temperature value of Ar and CNT during production run; The average temperature of CNT and argon is fitted using fourth order polynomial.

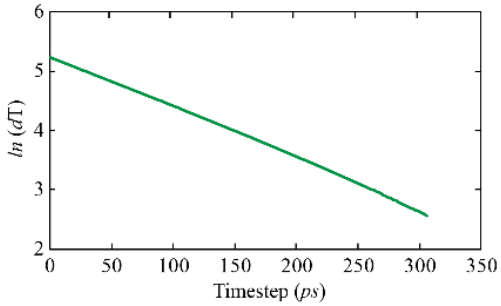

Fig. 5. Logarithmic decay in temperature difference of Ar and CNT during production run.

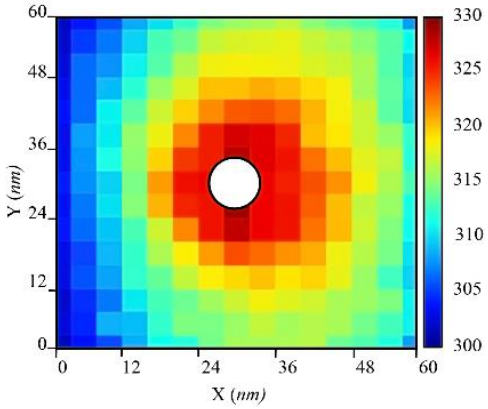

Fig. 6. Contour plot of temperature (K) distribution in argon flow over a CNT at steady state condition.

3.1 Computation of Interfacial Resistance

To compute the interfacial resistance between the argon atoms and carbon nanotube, a non-equilibrium molecular dynamics simulation have been performed. Figure 4 shows the instantaneous temperature variation of argon atoms and the carbon nanotube with respect to the simulation time. The average temperature variation of CNT and argon atoms are fitted using fourth order polynomial as shown in Fig. 4. It is observed that the temperature difference between the argon and CNT is decaying exponentially. Initially, the temperature of CNT set to be 500 K and for argon is 300 K. Because of a large amount of energy in the carbon nanotube, it transfers heat to the surrounding argon atoms until both the temperature becomes equal, and the whole system becomes equilibrium condition.

Figure 5 shows the decay in the temperature difference of argon and carbon nanotube with the simulation time. The reciprocal of the slope of this graph signifies the time constant value. From the plot the time constant τ found to be 111.67 ps. So the thermal interfacial resistance found to be 19.6×10^{-8} m^2K/W . The value of thermal interfacial resistance from this study has good agreement with the computed values in the available literature (Singh, Unnikrishnan, Banerjee and Reddy, 2011).

3.2 Argon Flow over a Carbon Nanotube

The convective heat transfer analysis of argon flow around a single wall carbon nanotube is investigated with non-equilibrium molecular dynamics simulations. Figure 6 represents the temperature distribution in the simulation domain. At the inlet section, the temperature of the argon atom is 300 K. A heated carbon nanotube with a constant temperature of 600 K is placed at the geometric center of the simulation box. When the argon atoms are reaching to the CNT, they are bombarding with the carbon atoms. So the thermal energy from the carbon nanotube is transferring to the argon atoms.

Figure 7 represents the velocity profile of argon atoms at various section along its length. At the inlet section, the velocity profile is uniform with a magnitude around 15 m/s. Up to the length of L = 10 A°, the velocity profile is uniform. Beyond this section, the shape of the velocity profile is deviating from the uniform flow. The collision of fast-moving argon atoms with the carbon atoms results in an opposite force to the argon atoms which is the reason for a deviated profile at the left side sections of the carbon nanotube. When argon atoms are crossing the carbon nanotube the center line velocity decreasing further to a low value and this loss is compensated to the argon atoms in the upper and lower layer regions by energy transfer.

Figure 8 indicates the fluctuations of the heat transfer coefficient (h) values with respect to timestep. This graph is plotted during the production run, i.e after the steady state condition. It is found that the heat transfer coefficient is fluctuating from a mean value. The mean value from these fluctuations approximated as the average value of heat transfer coefficient of this case. The heat transfer coefficient for argon flow around a single wall carbon nanotube is found to be 0.493×10^8 W/m2K.

3.3 Argon Flow over a Carbon Nanotube Arrays

Figure 9 represents the temperature distribution in 90° and 45° configurations. The maximum temperature of argon atoms attained by the heat transfer from carbon nanotube to the argon atoms is

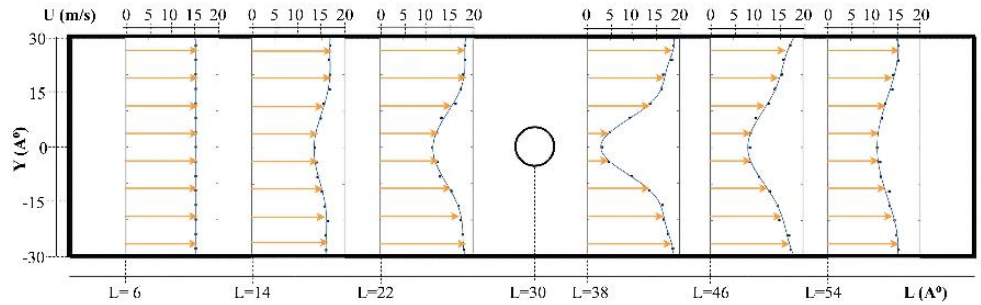

Fig. 7. Steady state velocity profile at various sections along the flow direction: Flow over a single CNT.

almost equal in both the configuration, it is around 333 K. The temperature distributions are almost symmetrical in both the cases as expected. For finding out the best configuration in terms of heat transfer rate, the heat transfer coefficient has to compute from the temperature distribution.

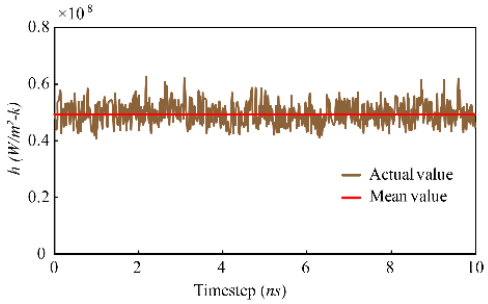

Fig. 8. Heat transfer co-efficient fluctuation with timestep during data extraction at steady state condition.

Figure 10 represents the velocity profile at various sections along the length of the simulation domain. The velocity profile of the 90° configuration is symmetric about y = 0 axis, at any cross-section along its length. But in the case of 45° configuration, the velocity profile is not symmetric. The amount of heat transfer rate strongly depends on the velocity of the fluid. A uniform velocity profile is supplied to the inlet section, but the velocity profile is varying in the whole domain because of momentum exchange between the atoms. Sum of the sine function is used for fitting the velocity profile in both the cases.

There are different parameters affecting the heat transfer coefficient values. It mainly depends upon the density of the fluid, temperature difference between CNT and surrounding fluid, the velocity of the fluid etc. Table 1 compares the values of heat transfer coefficient with different configurations. The heat transfer coefficient value of CNT pairs (1,3) and (2,4) are same in 90° configuration, be-cause of the symmetry in the configuration. But for the 45° configuration, heat transfer coefficient values are different for each nanotube. It is found that there is a slight increase in the heat transfer coefficient in the case of 45° configuration as compared with the 90° configuration. In the 45°, the flow velocity is slightly smaller, which leads to more interfacial exposure time. In the nano-scale configuration, since the surface to volume ratio is very large, the increase in interfacial exposure time lead to increase in the heat transfer rate.

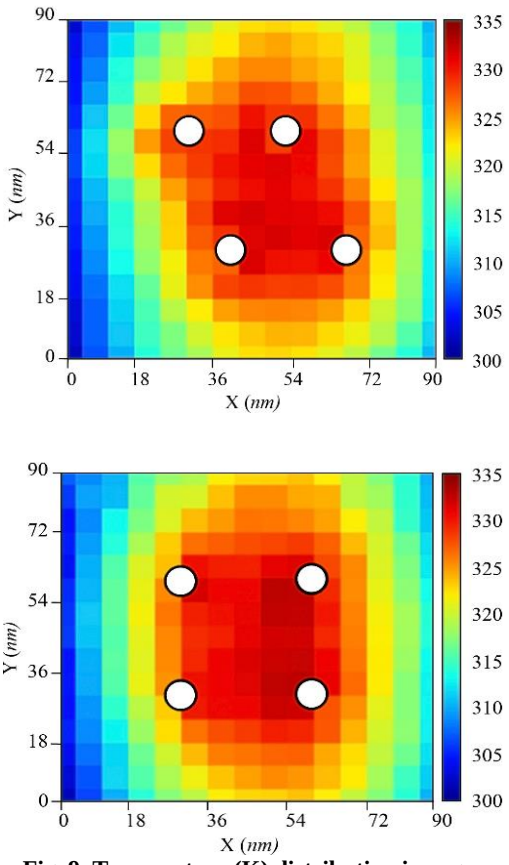

Fig. 9. Temperature (K) distribution in argon flow over a CNT arrays at steady state condition for two different configurations. Top: 45° configuration and bottom: 90◦ configuration.

4. CONCLUSIONS

A methodology in molecular dynamics simulations has presented in this article for investigating the steady-state convective heat transfer through the unconfined channel. With this methodology, the conventional periodic boundary condition in molecular dynamics flow simulations can be altered to a quasi-periodic boundary condition. It means particles will recycle from the outlet to inlet as like

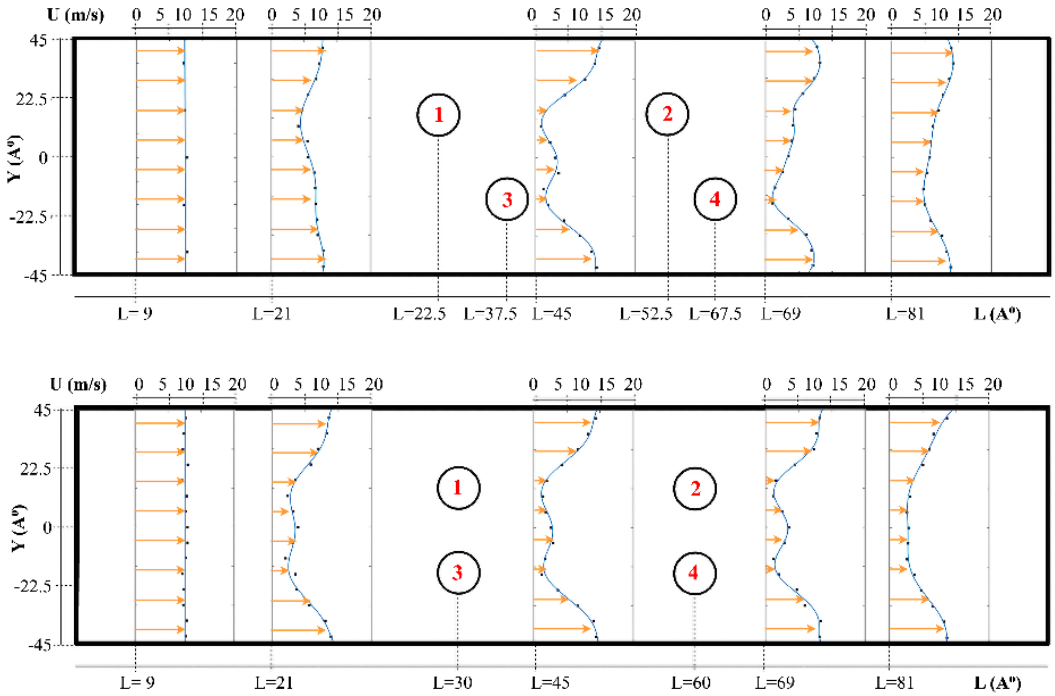

Fig. 10. Steady state velocity profile at various sections along the flow direction: Top: 45° configuration and bottom: 90° configuration.

in periodic boundary condition, but it maintains same inlet condition throughout the simulation. So, the temperature and velocity distribution at the inlet section will be maintained as same. It is achieved by constructing extra three artificial filters between the outlet and inlet section, which are not part of the actual system. These filters help to remove the past history of recycled particles.

Table 1 Comparison of Heat transfer coefficient in each CNTs of 45° and 90° configuration

CNT Position	Heat transfer coefficient ($\times 10^8 W/m^2K$)	
	90°	45°
CNT 1	1.84	1.83
CNT 2	1.96	1.96
CNT 3	1.84	1.91
CNT 4	1.96	2.05
Average Value	1.9000	1.9375

The convective heat transfer investigation on argon flow over the carbon nanotube and flow around the different configurations of CNT arrays have been considered for this research. Added to this, a non-equilibrium molecular simulation for the calculation of thermal interfacial resistance between argon atoms and nanotubes also considered. The value of thermal interfacial resistance found to be 19.6×10^{-8} m^2K/W, which is matching with the literature. The temperature distribution, velocity distribution and heat transfer coefficient values are considered in the convective heat transfer analysis. The heat transfer coefficient in all the cases is found to be in the order of 10^8 W/m2K. From the comparison of different CNT arrays configurations, it is found that a slight increase in the heat transfer coefficient value in the case of 45° configuration as compared with 90° configuration. The increase in heat transfer co-efficient can be attributed to the increase in the interfacial exposure time.

The major objective of this research was to develop a methodology in MD for simulating the forced convective steady flow through the unconfined channel. This methodology can be accurately applied even in the case of a confined channel. Molecular simulations can be carried out with realistic fluids and realistic velocity for actual understanding of heat transfer enhancement in nano-scale level.

ACKNOWLEDGEMENT

The authors are acknowledging to the High Performance Computing Laboratory at the Indian Institute of Technology Gandhinagar, India for the computational support.

REFERENCES

Alexiadis, A. and S. Kassinos (2008). Molecular simulation of water in carbon nanotubes. *Chemical Reviews* 108(12), 5014–5034.

Allen, M. P. and D. J. Tildesley (1989). Computer simulation of liquids. Oxford University Press.

Balandin, A. A. (2011). Thermal properties of graphene and nanostructured carbon materials. *Nature Materials* 10(8), 569.

Barber, J., D. Brutin and L. Tadrist (2011). A review

on boiling heat transfer enhancement with nanofluids. *Nanoscale Research Letters* 6(1), 1–16.

Barisik, M. and A. Beskok (2012). Boundary treatment effects on molecular dynamics simulations of interface thermal resistance. *Journal of Computational Physics* 231(23), 7881–7892.

Berber, S., Y.-K. Kwon and D. Tománek (2000). Unusually high thermal conductivity of carbon nanotubes. *Physical Review Letters* 84(20), 4613.

Berendsen, H. J., J. v. Postma, W. F. van Gunsteren, A. DiNola and J. Haak (1984). Molecular dynamics with coupling to an external bath. *The Journal of Chemical Physics* 81(8), 3684–3690.

Clancy, T. C. and T. S. Gates (2006). Modeling of interfacial modification effects on thermal conductivity of carbon nanotube composites. *Polymer* 47(16), 5990–5996.

Ge, S., Y. Gu and M. Chen (2015). A molecular dynamics simulation on the convective heat transfer in nanochannels. *Molecular Physics* 113(7), 703–710.

Heyes, D. M. (1994). Pressure tensor of partial-charge and point-dipole lattices with bulk and surface geometries. *Physical Review* B 49(2), 755.

Ho, C., B. Chen, M. Wen, T. Yang and Y. Lee (2016). Investigation into heat transfer characteristics in carbon nanotube using nanoscale thermal transport model. *Journal of Nanoscience and Nanotechnology* 16(9), 9268–9272.

Huxtable, S. T., D. G. Cahill, S. Shenogin, L. Xue, R. Ozisik, P. Barone, M. Usrey, M. S. Strano, G. Siddons, M. Shim, et al.(2003). Interfacial heat flow in carbon nanotube suspensions. *Nature Materials* 2(11), 731–734.

Incropera, F. (2007). *Fundamentals of Heat and Mass Transfer*. John Wiley.

Jones, J. E. (1924). On the determination of molecular fields II. from the equation of state of a gas. *In Proceedings of the Royal Society of London A: Mathematical, Physical and Engineering Sciences* 106, 463–477.

Kandlikar, S. G. (2005). High flux heat removal with microchannelsa roadmap of challenges and opportunities. *Heat Transfer Engineering* 26(8), 5–14.

Karayiannis, T. and M. Mahmoud (2017). Flow boiling in microchannels: Fundamentals and applications. *Applied Thermal Engineering* 115, 1372–1397.

Kim, P., L. Shi, A. Majumdar and P. L. McEuen (2001). Thermal transport measurements of individual multiwalled nanotubes. *Physical Review Letters* 87(21), 215502.

Liu, C., H.-B. Fan, K. Zhang, M. M. Yuen and Z. Li (2010). Flow dependence of interfacial thermal resistance in nanochannels. *The Journal of Chemical physics* 132(9), 094703.

Markvoort, A. J., P. A. J. Hilbers and S. V. Nedea (2005). Molecular dynamics study of the influence of wall-gas interactions on heat flow in nanochannels. *Physical Review E* 71, 066702.

Martínez, L., R. Andrade, E. G. Birgin, and J. M. Martínez (2009). Packmol: a package for building initial configurations for molecular dynamics simulations. *Journal of Computational Chemistry* 30(13), 2157–2164.

Merabia, S., P. Keblinski, L. Joly, L. J. Lewis, and J.-L. Barrat (2009). Critical heat flux around strongly heated nanoparticles. *Physical Review E* 79(2), 021404.

Plimpton, S., P. Crozier and A. Thompson (2007). Lammps-large-scale atomic/molecular massively parallel simulator. Sandia National Laboratories 18.

Prabha, S. K. and S. P. Sathian (2012). Molecular-dynamics study of poiseuille flow in a nanochannel and calculation of energy and momentum accommodation coefficients. *Physical Review E* 85(4), 041201.

Rabani, R., G. Heidarinejad, J. Harting and E. Shirani (2018). Interplay of confinement and density on the heat transfer characteristics of nanoscale-confined gas. *International Journal of Heat and Mass Transfer* 126, 331–341.

Sääskilahti, K., J. Oksanen, S. Volz and J. Tulkki (2015). Frequency-dependent phonon mean free path in carbon nanotubes from nonequilibrium molecular dynamics. *Physical Review B* 91(11), 115426.

Schneider, T. and E. Stoll (1978). Molecular-dynamics study of a three-dimensional one-component model for distortive phase transitions. *Physical Review B* 17(3), 1302.

Singh, N., V. Unnikrishnan, D. Banerjee and J. Reddy (2011). Analysis of thermal inter-facial resistance between nanofins and various coolants. *International Journal for Computational Methods in Engineering Science and Mechanics* 12(5), 254–260.

Stuart, S. J., A. B. Tutein and J. A. Harrison (2000). A reactive potential for hydrocarbons with intermolecular interactions. *The Journal of Chemical Physics* 112(14), 6472–6486.

Tuckerman, D. B. and R. F. W. Pease (1981). High-performance heat sinking for vlsi. *IEEE Electron Device Letters* 2(5), 126–129.

Van Gunsteren, W. F., P. K. Weiner and A. J. Wilkinson (2013). *Computer simulation of biomolecular systems: theoretical and experimental applications*, Volume 3. Springer Science & Business Media.

Wu, H. and P. Cheng (2003). Friction factors in smooth trapezoidal silicon microchannels with different aspect ratios. *International Journal of Heat and Mass Transfer* 46(14), 2519 – 2525.

Xu, Z. and M. J. Buehler (2009). Nanoengineering heat transfer performance at carbon nanotube interfaces. ACS nano 3(9), 2767–2775.

You, S. M., J. H. Kim and K. H. Kim (2003). Effect of nanoparticles on critical heat flux of water in pool boiling heat transfer. *Applied Physics Letters* 83(16), 3374–3376.

Yu, C., L. Shi, Z. Yao, D. Li and A. Majumdar (2005). Thermal conductance and thermopower of an individual single-wall carbon nanotube. *Nano letters* 5(9), 1842–1846.

Yu, J., J. G. Shapter, J. S. Quinton, M. R. Johnston and D. A. Beattie (2007). Direct attachment of well-aligned single-walled carbon nanotube architectures to silicon (100) surfaces: a simple approach for de-vice assembly. *Physical Chemistry Chemical Physics* 9(4), 510–520.

Zhang, P., P. Yuan, X. Jiang, S. Zhai, J. Zeng, Y. Xian, H. Qin and D. Yang (2018). A theoretical review on interfacial thermal transport at the nanoscale. *Small* 14(2), 1702769.